# Calculations executed for the 3-bladed rotor of the VIRYA-3.6PC windmill ($\lambda_d$ = 4.5, galvanised steel blades) driving the VIRYA-4.2 PM-generator for 26 V star or driving a centrifugal pump through a rectangular gear box and a vertical shaft in the tower. Description of the pitch control safety system

ing. A. Kragten

April 2018

KD 654



Engineering office Kragten Design
Populierenlaan 51
5492 SG Sint-Oedenrode
The Netherlands
telephone: +31 413 475770
e-mail: info@kdwindturbines.nl
website: www.kdwindturbines.nl

Contains page

## 1 Introduction

The 3-bladed VIRYA-3.6PC windmill has a rotor with a pitch control (PC) safety system. The VIRYA-3.6PC is primary designed to be coupled to the VIRYA-4.2 PM-generator rectified in star for 24 V battery charging. The estimated characteristics of this generator for 26 V star are given in chapter 5 of report KD 200 (ref. 1). However, the VIRYA-3.6PC rotor can also be used to replace the 4-bladed VIRYA-3.6 rotor if one prefers a rotor with a pitch control system to limit the rotational speed and thrust. No eccentricity is needed if a pitch control safety system is used and now the rotor shaft can be coupled to the vertical shaft by a standard rectangular gear box. The 4-bladed VIRYA-3.6 is used to drive a centrifugal pump using a Polycord transmission with a round string in the windmill head and a vertical shaft in the tower. The VIRYA-3.6 is described in report KD 653 (ref. 2). As the rotational speed of the vertical shaft of the VIRYA-3.6PC will become higher, a thicker shaft may be needed to prevent instability at maximum rotational speed.

The VIRYA-3.6PC is meant for use in developing countries and western countries. The VIRYA-3.6PC windmill has a 3-bladed rotor with galvanised steel blades but if available, stainless steel can also be used.

The tower is the same as the 12 m tower of the VIRYA-4.2. As an alternative, the tubular tower as described in report KD 582 (ref. 3) can be used. Use of the VIRYA-3.6PC for driving a centrifugal pump requires a special lattice tower with integrated vertical shaft. The head is totally different and has a double vane to keep the rotor in the wind.

## 2 Description of the rotor of the VIRYA-3.6PC windmill

The 3-bladed rotor of the VIRYA-3.6PC windmill has a diameter D = 3.6 m and a design tip speed ratio $\lambda_d = 4.5$. The rotor has blades with a constant chord and is provided with a 7.14 % cambered airfoil. Aerodynamic characteristics of a 7.14 % cambered airfoil are given in report KD 398 (ref. 4). A blade is made of a steel strip with dimensions of 208 * 1250 * 3 mm and twelve blades can be made from a standard galvanised sheet size 1.25 * 2.5 m with only minimal losses. Because the blade is cambered, the chord c is a little less than the blade width, resulting in c = 205 mm = 0.205 m.

A design tip speed ratio $\lambda_d = 4.5$ is rather high for a rotor with 7.14 % cambered blades and the rotor therefore can be rather noisy, especially if it is running at a higher tip speed ratio than $\lambda_d$. So the VIRYA-3.6PC windmill should only be used at places where some noise production isn't a problem.

A blade is connected to the hub plate by a round 20 mm stainless steel blade shaft. A cambered strip size 210 * 50 * 6 mm is welded exactly square to the outer end of the blade shaft and the blade is connected to this strip by three M10 bolts. The axis of the blade shaft corresponds to the quart cord point of the airfoil and the pitch movement is steered by the aerodynamic moment. A blade shaft turns in two needle bearings and one stainless steel thrust bearing. A needle bearing is pressed in a bearing housing. The six bearing housings are bolted to the hub sheet. The hub sheet is bolted to the hub by three M12 bolts The pitch control system is described in detail in chapter 6. A blade shaft is chosen that long that the rotor diameter is 3.6 m. The overlap in between a blade and the cambered strip is 0.05 m resulting in a free blade length of 1.2 m. This blade length in combination with a design tip speed ratio $\lambda_d = 4.5$ and a blade thickness of 3 mm is expected to be enough to prevent flutter of the blade at high rotational speeds.

The hub plate is made of 6 mm stainless steel sheet and bolted to the hub by three M12 bolts. The hub is made of 80 mm round stainless steel bar with a length of 58 mm and with a tapered hole in the centre for connection to the 35 mm generator shaft. The hub is pulled on the tapered shaft end of the generator by one central bolt M16. A sketch of the rotor is given in figure 1.

## 3 Calculation of the rotor geometry

The rotor geometry is determined using the method and the formulas as given in report KD 35 (ref. 5). This report (KD 654) has its own formula numbering. Substitution of $\lambda_d = 4.5$ and R = 1.8 m in formula (5.1) of KD 35 gives:

$$\lambda_{r\,d} = 2.5 * r \qquad (-) \qquad (1)$$

Formula's (5.2) and (5.3) of KD 35 stay the same so:

$$\beta = \phi - \alpha \qquad (°) \qquad (2)$$

$$\phi = 2/3 \arctan 1 / \lambda_{r\,d} \qquad (°) \qquad (3)$$

Substitution of B = 3 and c = 0.205 m in formula (5.4) of KD 35 gives:

$$C_l = 40.866\ r\ (1 - \cos\phi) \qquad (-) \qquad (4)$$

Substitution of V = 5 m/s and c = 0.205 m in formula (5.5) of KD 35 gives:

$$R_{e\,r} = 0.684 * 10^5 * \sqrt{(\lambda_{r\,d}^2 + 4/9)} \qquad (-) \qquad (5)$$

The blade is calculated for eleven stations A till K which have a distance of 0.12 m of one to another. Station F corresponds to the end of the blade shaft. The blade has a constant chord and the calculations therefore correspond with the example as given in chapter 5.4.2 of KD 35. This means that the blade is designed with a low lift coefficient at the tip and with a high lift coefficient at the root. First the theoretical values are determined for $C_l$, $\alpha$ and $\beta$ and next $\beta$ is linearised such that the twist is constant and that the linearised values for the outer part of the blade correspond as good as possible with the theoretical values. The result of the calculations is given in table 1.

The aerodynamic characteristics of a 7.14 % cambered airfoil are given in report KD 398 (ref. 4). The Reynolds values for the stations are calculated for a wind speed of 5 m/s because this is a reasonable wind speed for a site with a good wind regime. Those airfoil Reynolds numbers are used which are lying closest to the calculated values.

| station | r (m) | $\lambda_{rd}$ (-) | $\phi$ (°) | c (m) | $C_{l\,th}$ (-) | $C_{l\,lin}$ (-) | $R_{e\,r} * 10^{-5}$ V = 5 m/s | $R_e * 10^{-5}$ 7.14 % | $\alpha_{th}$ (°) | $\alpha_{lin}$ (°) | $\beta_{th}$ (°) | $\beta_{lin}$ (°) | $C_d/C_{l\,lin}$ (-) |
|---|---|---|---|---|---|---|---|---|---|---|---|---|---|
| A | 1.8 | 4.5 | 8.4 | 0.205 | 0.78 | 0.82 | 3.11 | 3.4 | 0.0 | 0.4 | 8.4 | 8.0 | 0.036 |
| B | 1.68 | 4.2 | 8.9 | 0.205 | 0.83 | 0.86 | 2.91 | 3.4 | 0.5 | 0.9 | 8.4 | 8.0 | 0.032 |
| C | 1.56 | 3.9 | 9.6 | 0.205 | 0.89 | 0.89 | 2.71 | 2.5 | 1.6 | 1.6 | 8.0 | 8.0 | 0.032 |
| D | 1.44 | 3.6 | 10.3 | 0.205 | 0.96 | 0.95 | 2.50 | 2.5 | 2.5 | 2.3 | 7.8 | 8.0 | 0.032 |
| E | 1.32 | 3.3 | 11.2 | 0.205 | 1.03 | 1.04 | 2.30 | 2.5 | 3.1 | 3.2 | 8.1 | 8.0 | 0.038 |
| F | 1.20 | 3.0 | 12.3 | 0.205 | 1.12 | 1.15 | 2.10 | 2.5 | 4.0 | 4.3 | 8.3 | 8.0 | 0.042 |
| G | 1.08 | 2.7 | 13.5 | 0.205 | 1.23 | 1.18 | 1.90 | 1.7 | 6.1 | 5.5 | 7.4 | 8.0 | 0.050 |
| H | 0.96 | 2.4 | 15.1 | 0.205 | 1.35 | 1.32 | 1.70 | 1.7 | 7.8 | 7.1 | 7.3 | 8.0 | 0.090 |
| I | 0.84 | 2.1 | 17.0 | 0.205 | 1.50 | 1.40 | 1.51 | 1.7 | - | 9.0 | - | 8.0 | 0.116 |
| J | 0.72 | 1.8 | 19.4 | 0.205 | 1.67 | 1.44 | 1.31 | 1.2 | - | 11.4 | - | 8.0 | 0.145 |
| K | 0.6 | 1.5 | 22.5 | 0.205 | 1.86 | 1.30 | 1.12 | 1.2 | - | 14.5 | - | 8.0 | 0.230 |

table 1 Calculation of the blade geometry of the VIRYA-3.6PC rotor

No value for $\alpha_{th}$ and therefore for $\beta_{th}$ is found for stations I, J and K because the required $C_l$ values can't be generated.

The theoretical blade angle $\beta_{th}$ for stations A to H varies in between 8.4° and 7.3°. If a constant blade angle of 8° is chosen, the linearised angle of attack $\alpha_{lin}$ differs only a little from the theoretical value $\alpha_{th}$ for the most important outer side of the blade.

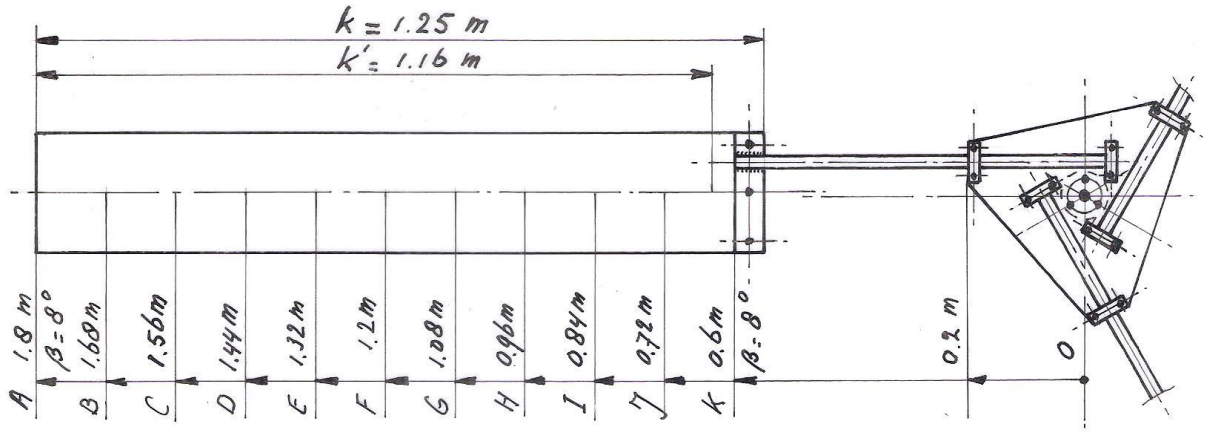


fig. 1 Sketch VIRYA-3.6PC rotor

## 4 Determination of the $C_p$-$\lambda$ and the $C_q$-$\lambda$ curves

The determination of the $C_p$-$\lambda$ and $C_q$-$\lambda$ curves is given in chapter 6 of KD 35. The average $C_d/C_l$ ratio for the most important outer part of the blade is about 0.038. Figure 4.7 of KD 35 (for B = 3) and $\lambda_{opt}$ = 4.5 and $C_d/C_l$ = 0.038 gives $C_{p\ th}$ = 0.435 (interpolation in between the lines for $C_d/C_l$ = 0.03 and $C_d/C_l$ = 0.05). The blade is stalling in between station J and K. Therefore not the whole blade length k = 1.25 m, but only the part up to 0.04 m outside station K is used for the calculation of the $C_p$. This gives an effective blade length k' = 1.16 m.

Substitution of $C_{p\ th}$ = 0.435, R = 1.8 m and effective blade length k = k' = 1.16 m in formula 6.3 of KD 35 gives $C_{p\ max}$ = 0.38. $C_{q\ opt} = C_{p\ max} / \lambda_{opt}$ = 0.38 / 4.5 = 0.0844.
Substitution of $\lambda_{opt} = \lambda_d$ = 4.5 in formula 6.4 of KD 35 gives $\lambda_{unl}$ = 7.2.
The starting torque coefficient is calculated with formula 6.12 of KD 35 which is given by:

$$C_{q\ start} = 0.75 * B * (R - \tfrac{1}{2}k) * C_l * c * k / \pi R^3 \qquad (-) \qquad (6)$$

The blade angle is 8° for the whole blade. For a non rotating rotor the average angle of attack $\alpha$ is therefore 90° - 8° = 82°. The estimated $C_l$-$\alpha$ curve for large values of $\alpha$ is given as figure 5 of KD 398. For $\alpha$ = 82° it can be read that $C_l$ = 0.27. The whole blade is stalling during starting and therefore now the whole blade length k = 1.25 m is taken.

Substitution of B = 3, R = 1.8 m, k = 1.25 m, $C_l$ = 0.27 and c = 0.205 m in formula 6 gives that $C_{q\ start}$ = 0.010. For the ratio in between the starting torque and the optimum torque we find that it is 0.010 / 0.0844 = 0.119. This is good for a rotor with a design tip speed ratio of 4.5. The starting wind speed $V_{start}$ of the rotor is calculated with formula 8.6 of KD 35 which is given by:

$$V_{start} = \sqrt{\left(\frac{Q_s}{C_{q\ start} * \tfrac{1}{2}\rho * \pi R^3}\right)} \qquad (m/s) \qquad (7)$$

The unloaded sticking torque $Q_s$ of the PM-generator has been measured for star and for delta rectification (see fig. 1 KD 200). It is 0.9 Nm for stand still position. It rises much faster at increasing rotational speed for delta than for star rectification because higher harmonic currents can circulate in the winding for delta rectification.

But for the VIRYA-3.6PC, the winding is rectified in star for 24 V battery charging. If the generator is used as a brake, the star point should be short-circuited too because this gives a larger breaking torque. Substitution of $Q_s = 0.9$ Nm, $C_{q\ start} = 0.010$, $\rho = 1.2$ kg/m$^3$ and $R = 1.8$ m in formula 7 gives that $V_{start} = 2.9$ m/s. This is acceptable low for a 3-bladed rotor with a design tip speed ratio of 4.5. The P-n curve of the rotor for $V = 2.9$ m/s is rising faster than the unloaded P-n curve of the generator for star rectification and the rotor will therefore really start at a wind speed of 2.9 m/s.

In chapter 6.4 of KD 35 it is explained how rather accurate $C_p$-$\lambda$ and $C_q$-$\lambda$ curves can be determined if only two points of the $C_p$-$\lambda$ curve and one point of the $C_q$-$\lambda$ curve are known. The first part of the $C_q$-$\lambda$ curve is determined according to KD 35 by drawing an S-shaped line which is horizontal for $\lambda = 0$.

Kragten Design developed a method with which the value of $C_q$ for low values of $\lambda$ can be determined (see report KD 97 ref. 6). With this method, it can be determined that the $C_q$-$\lambda$ curve is directly rising for low values of $\lambda$ if a 7.14 % cambered sheet airfoil is used. This effect has been taken into account and the estimated $C_p$-$\lambda$ and $C_q$-$\lambda$ curves for the VIRYA-3.6PC rotor are given in figure 2 and 3.

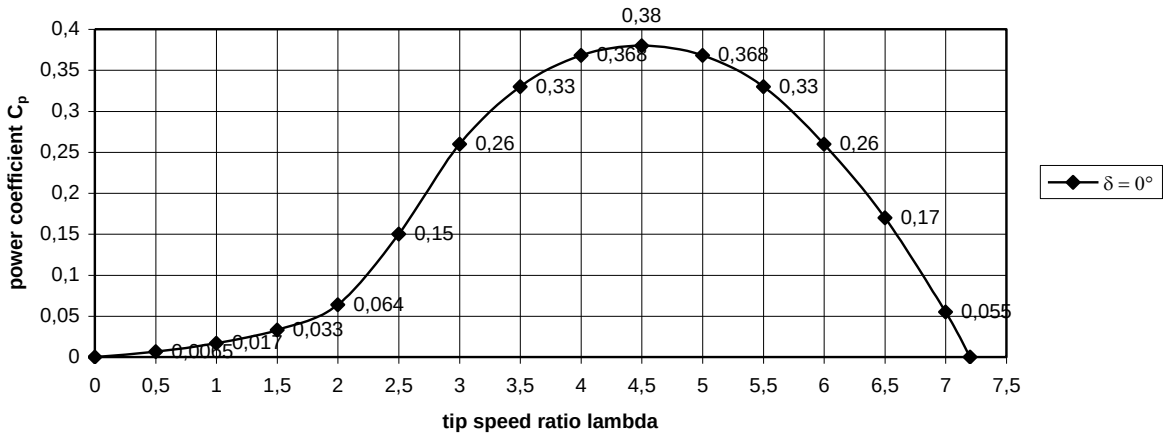


fig. 2 Estimated $C_p$-$\lambda$ curve for the VIRYA-3.6PC rotor for the wind direction perpendicular to the rotor ($\delta = 0°$)

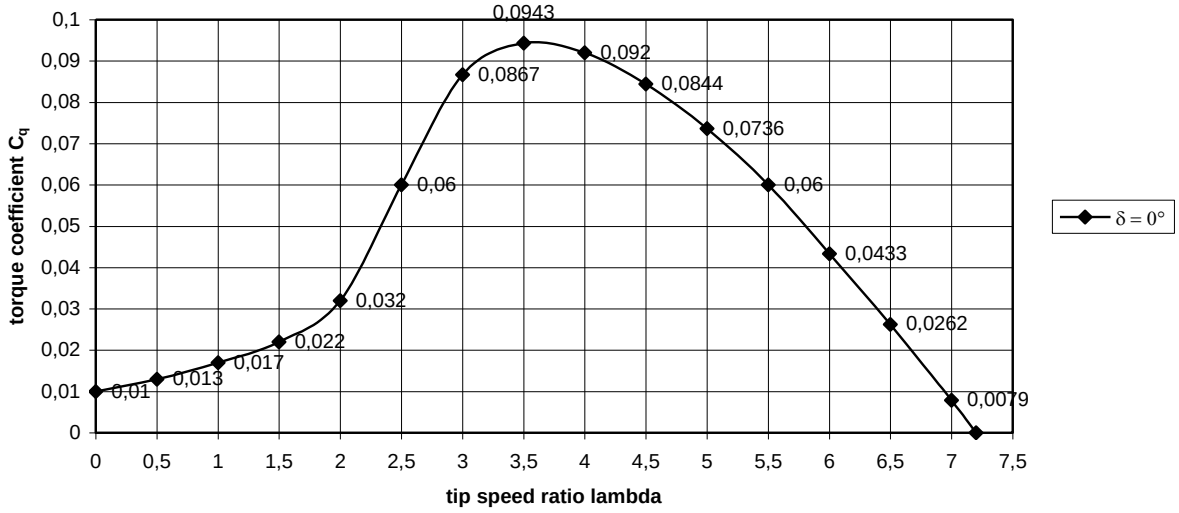


fig. 3 Estimated $C_q$-$\lambda$ curve for the VIRYA-3.6PC rotor for the wind direction perpendicular to the rotor ($\delta = 0°$)

## 5 Determination of the P-n curves and the $P_{el}$-V curve

The determination of the P-n curves of a windmill rotor is described in chapter 8 of KD 35. One needs a $C_p$-$\lambda$ curve of the rotor and the characteristics of the safety system together with the formulas for the power P and the rotational speed n. The $C_p$-$\lambda$ curve is given in figure 2. A pitch control safety system changes the shape of the P-n curves above the rotational speed for which the safety system becomes active. At this moment the effect of the safety system is not yet taken into account but it will be discussed in chapter 6. It is assumed that the rotor is perpendicular to the wind so the formulas for P and n are used which are given in chapter 4.1 of KD 35. The P-n curves are determined for wind the speeds 3, 4, 5, 6, 7, 8, 9 and 10 m/s.

Substitution of R = 1.8 m in formula 4.8 of KD 35 gives:

$$n = 5.3052 * \lambda * V \qquad \text{(rpm)} \qquad (8)$$

Substitution of $\rho = 1.2$ kg / $m^3$ and R = 1.8 m in formula 4.1 of KD 35 gives:

$$P = 6.1073 * C_p * V^3 \qquad \text{(Nm)} \qquad (9)$$

The P-n curves are determined for $C_p$ values belonging to $\lambda$ is 2.5, 3.5, 4.5, 5.5, 6.5 and 7.2 (see figure 2). For a certain wind speed, for instance V = 3 m/s, related values of $C_p$ and $\lambda$ are substituted in formula 8 and 9 and this gives the P-n curve for that wind speed. The result of the calculations is given in table 2.

| | | V = 3 m/s | | V = 4 m/s | | V = 5 m/s | | V = 6 m/s | | V = 7 m/s | | V = 8 m/s | | V = 9 m/s | | V = 10 m/s | |
|---|---|---|---|---|---|---|---|---|---|---|---|---|---|---|---|---|---|
| $\lambda$ (-) | $C_p$ (-) | n (rpm) | P (W) | n (rpm) | P (W) | n (rpm) | P (W) | n (rpm) | P (W) | n (rpm) | P (W) | n (rpm) | P (W) | n (rpm) | P (W) | n (rpm) | P (W) |
| 2.5 | 0.15 | 39.8 | 24.7 | 53.1 | 58.6 | 66.3 | 114.5 | 79.6 | 197.9 | 92.8 | 314.2 | 106.1 | 469.0 | 119.4 | 667.8 | 132.6 | 916.1 |
| 3.5 | 0.33 | 55.7 | 54.4 | 74.3 | 129.0 | 92.8 | 251.9 | 111.4 | 435.3 | 130.0 | 691.3 | 148.5 | 1032 | 167.1 | 1469 | 185.7 | 2015 |
| 4.5 | 0.38 | 71.6 | 62.7 | 95.5 | 148.5 | 119.4 | 290.1 | 143.2 | 501.3 | 167.1 | 796.0 | 191.0 | 1188 | 214.9 | 1692 | 238.7 | 2321 |
| 5.5 | 0.33 | 87.5 | 54.4 | 116.7 | 129.0 | 145.9 | 251.9 | 175.1 | 435.3 | 204.3 | 691.3 | 233.4 | 1032 | 262.6 | 1469 | 291.8 | 2015 |
| 6.5 | 0.17 | 103.5 | 28.0 | 137.9 | 66.4 | 172.4 | 129.8 | 206.9 | 224.3 | 241.4 | 356.1 | 275.9 | 531.6 | 310.4 | 756.9 | 344.8 | 1038 |
| 7.2 | 0 | 114.6 | 0 | 152.8 | 0 | 191.0 | 0 | 229.2 | 0 | 267.4 | 0 | 305.6 | 0 | 343.8 | 0 | 382.0 | 0 |

table 2 Calculated values of n and P as a function of $\lambda$ and V for the VIRYA-3.6PC rotor

The calculated values for n and P are plotted in figure 4. The optimum cubic line which is going through the points of maximum power, is also drawn in figure 4.

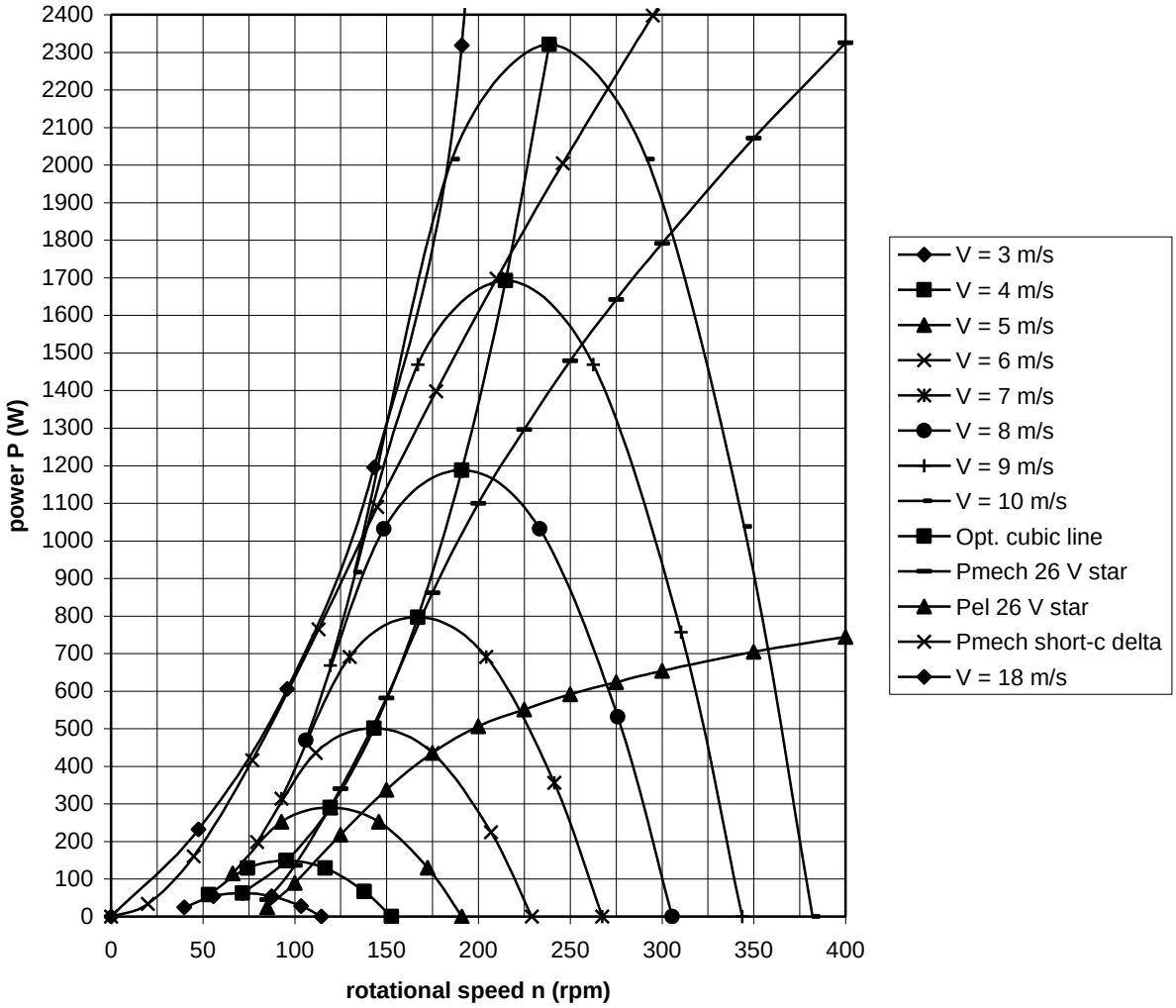


fig. 4 P-n curves of the VIRYA-3.6PC rotor, optimum cubic line and estimated $P_{mech}$-n and $P_{el}$-n curves of the generator for 26 V star

The VIRYA-4.2 PM-generator has been measured for different constant DC voltages for rectification in star. However, it hasn't been measured for a voltage of 26 V which is the average voltage for a 24 V battery. But the estimated characteristics for 26 V star are derived in chapter 5 of report KD 200 (ref. 1).

The $P_{mech}$-n and the $P_{el}$-n curve for 26 V star as derived in chapter 5 of KD 200, are copied in figure 4. In figure 4 it can be seen that the matching is very good for wind speeds in between 4 m/s and 8 m/s because the $P_{mech}$-n curve of the generator is lying very close to the optimum cubic line of the rotor. However, the efficiency of the generator for 26 V star is low at high powers and this results in a rather low $P_{el}$-n curve for higher rotational speeds.

The measured $P_{mech}$-n curve for short-circuit in delta as given in figure 5 of KD 200 has also been copied in figure 4. Short-circuit in delta is the same as short-circuit in star if the star point is short-circuited too. In figure 4 it can be seen that this line is about touching the P-n curve of the rotor for V = 8.5 m/s (not drawn) so this means that the generator should be used as a brake only for wind speeds lower than 8 m/s otherwise the rotor won't stop and the generator winding may burn! The P-n curve of the rotor for V = 18 m/s and for low values of $\lambda$ is also given in figure 4. This curve is about touching the P-n curve of the generator for short-circuit in delta. This means that the rotor starts rotating from stand still position at 18 m/s! So for high wind speeds, a braked rotor must be connected to the head (by a chain)!

The point of intersection of the $P_{mech}$-n curve of the generator with the P-n curve of the rotor for a certain wind speed, gives the working point for that wind speed. The electrical power $P_{el}$ for that wind speed is found by going down vertically from the working point up to the point of intersection with the $P_{el}$-n curve. The values of $P_{el}$ found this way for all wind speeds, are plotted in the $P_{el}$-V curve (see figure 5). The charging voltage at high powers will be somewhat higher than the average charging voltage of 26 V and therefore the generator efficiency will be somewhat higher too. This results in a somewhat higher electrical power. The $P_{el}$-V curve is corrected for this effect for high wind speeds.

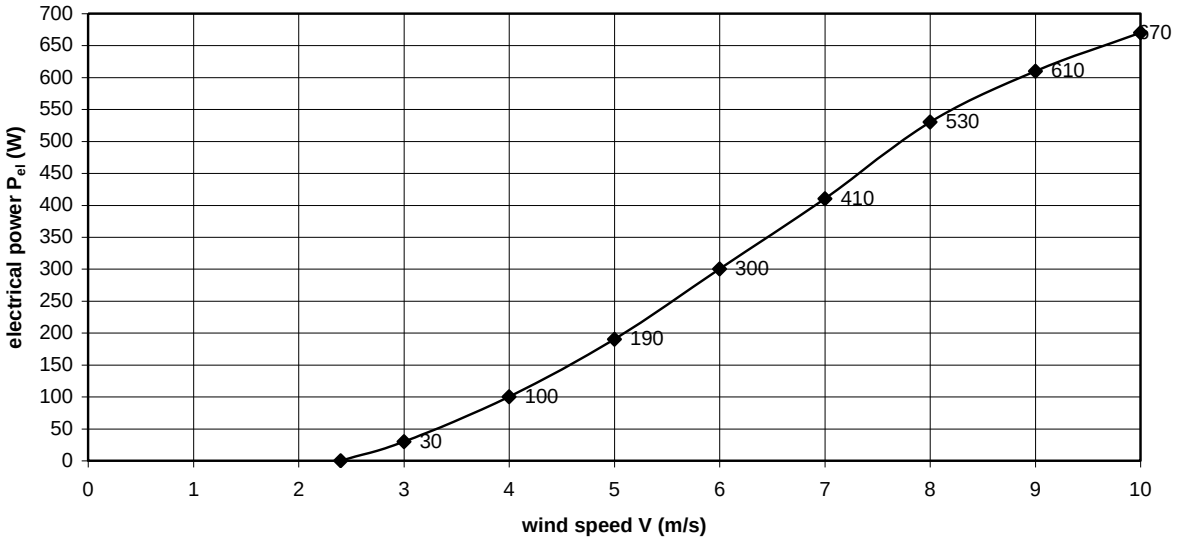


fig. 5 $P_{el}$-V curve of the VIRYA-3.6PC windmill for 24 V battery charging and for the VIRYA-4.2 PM-generator rectified in star

In figure 5 it can be seen that the supply of power already starts at a wind speed of 2.4 m/s. This is very low so the VIRYA-3.6PC with the VIRYA-4.2 generator can be used in regions with low wind speeds. However, this is only the case if the rotor is rotating. In chapter 3 it was calculated that the starting wind speed is 2.9 m/s so there is hysteresis in the $P_{el}$-V curve for wind speeds in between 2.4 and 2.9 m/s.

The generator efficiency at rotational speeds in between 100 rpm and 150 rpm, corresponding to wind speeds in between about 4 m/s and 6 m/s, is still rather high so the electrical power at these wind speeds is rather high. The maximum power is a 670 W which is a bit low for a windmill with 3.6 m rotor diameter. This rather low power is caused by the rather low generator efficiency at high rotational speeds for 26 V star. The pitch control safety system starts at a wind speed of 8 m/s. So the real $P_{el}$-V curve is flattened above this wind speed. The same generator is used in the VIRYA-4.2 but then for 48 V battery charging, so for an average charging voltage of 52 V star. Then the maximum power is about 1100 W.

## 6 Description of the pitch control mechanism

### 6.1 General aspects of pitch controls systems

The blade angle β is sometimes called the pitch angle. So a pitch control system is a safety system which uses variation of the blade angle to limit the maximum rotational speed and the maximum power. The limitation can be realised by two directions of blade rotation. Rotation of the blade to smaller blade angles is called negative pitch control or active stall. Rotation of the blade to larger blade angles is called positive pitch control.

Rotation of the blade to smaller blade angles results in increase of the angle of attack $\alpha$. At a certain value of $\alpha$, the maximum lift coefficient $C_{l\ max}$ is reached and this is the angle $\alpha_{st}$ where stalling starts. For higher angles $\alpha$, and so for smaller angles $\beta$, $C_l$ decreases somewhat but the drag coefficient $C_d$ increases strongly if $\alpha$ is higher than $\alpha_{st}$. At a certain angle $\beta$, the component of the drag opposed to the direction of rotation will become larger than the component of the lift in the direction of rotation (see KD 35 figure 4.4 and formula 4.14). This means that all generated power will be used to overcome the airfoil drag. So no mechanical power can be generated on the rotor shaft and this means that the rotor will slow down if the generator withdraws power from the rotor.

The VIRYA-3.6PC rotor is designed with a high lift coefficient at the blade root and a low lift coefficient at the blade tip. So the stalling point will move from the inside of the blade to the outside of the blade if the blade angle is decreased.

**Advantages of negative pitch control**

1) Only a rather small maximum decrease of the blade angle (about 10°, so $\beta$ = -2°) is needed to realise stalling for the almost the whole blade length.
2) A sudden wind gust results in a sudden increase of the angle of attack $\alpha$. So only a little variation in the blade angle is required to realise stalling for a large part of the blade length.
3) If variation of the blade angle is also used to increase the starting torque, one can go from a large blade angle at starting to a small blade angle at the normal design tip speed ratio and than to a negative blade angle at stalling, using one mechanism working in the same direction.

**Disadvantages of negative pitch control**

1) It results in increase of the rotor thrust especially at the blade tip.
2) A stalling blade may be rather noisy.
3) The aerodynamic moment is working in a direction which has a tendency to increase the blade angle. So a rather large pitch moment is needed to over power the aerodynamic moment. If this pitch moment is supplied by centrifugal weights, rather large weights will be needed.

Rotation of the blade to larger blade angles results in decrease of the angle of attack $\alpha$. A smaller angle $\alpha$ result in decrease of the lift coefficient and so in decrease of the generated torque. So if the generator loads the rotor with a certain torque, the rotational speed will decrease.

**Advantages of positive pitch control**

1) The aerodynamic moment works in a direction which has a tendency to increase the blade angle. So the aerodynamic moment can be used to activate the pitch control system. If the aerodynamic moment is not large enough, relative small centrifugal weight are needed to give some extra pitch moment.
2) This system results in decrease of the lift coefficient so in decrease of the rotor thrust and so in decrease of the forces on the tower and the foundation.
3) The rotor stops rotating for $\beta$ = 92° ($C_l$ = 0, $\alpha$ = -2°). So no brake is needed for $\beta$ = 92°.

**Disadvantages of positive pitch control**

1) A rather large increase of the blade angle of about 30° is needed (so $\beta_{max}$ = 38°) to limit the rotational speed enough at very high wind speeds.
2) A sudden wind gust results in a sudden increase of the angle of attack $\alpha$. So a large blade angle will be needed to realise a blade angle $\alpha$ which is small enough to compensate the wind gust.

Apart from aerodynamic forces and centrifugal forces also the force due to the weight of the centrifugal weights, is active. The direction of this force with respect to the position of the blade varies 360° during one blade rotation. This will cause some variation of the blade angle. To prevent this variation, it is necessary that the movements of all blades are synchronised by the pitch control mechanism if centrifugal weights are used for the pitch control system. However, if the pitch control system is only activated by the aerodynamic moment, the situation is different.

The aerodynamic moment for a certain blade section is determined by the relative wind speed W. The relative wind speed W is illustrated in figure 5.1 of KD 35 and is the vector sum of the local blade speed Ω * r and the absolute wind speed in the rotor plane 2/3 V (if the wake rotation is neglected). For rotors with a high design tip speed ratio like the VIRYA-3.6PC rotor, Ω * r is large with respect to 2/3 V which means that W is only a little larger than Ω * r. So even if the absolute wind speed isn't constant for the whole rotor plane, Ω * r will be almost constant for a certain value of r and this means that W will be almost constant for a certain rotational speed. This means that the increase of the blade angle will be the same for all three blades if the friction of the pitch control system is the same for each blade and so no synchronisation mechanism is required.

Pitch variation can be steered by the aerodynamic moment, by a pitch moment which is caused by centrifugal weights or by an external energy source. Modern very large 3-bladed windmills generally use an external source and a computer for each windmill. The pitch variation of all three blades is synchronised by a system of levers on each of the blade roots. The rotor shaft is hollow and contains a pin which is connected to the blade levers. The blades can rotate more than 90° if the pin is moved front- or backwards. The movement of the pin is caused by a hydraulic cylinder which is steered by the rotational speed or by the generated power. But any signal can be used to activate the pitch control system. The system can be used to stop the rotor for a positive blade angle of about 99°. It can also be used to facilitate starting, by slowly decreasing the blade angle if the rotor is accelerating.

An important disadvantage of this system is that it only works as long as energy is available to power the hydraulic system. If this energy is directly taken from the grid, the whole system will fail if the grid falls off. So some back up power is needed. Another disadvantage is that the system only works if the computer and the hydraulics work. If there is a break down in one of these systems, the pitch control system will fail and the rotor may rotate that fast that it can be destroyed. This system is certainly too complicated and too expensive for the VIRYA-3.6PC windmill.

### 6.2 Choices made for the pitch control system of the VIRYA-3.6PC

It is expected that certain developing countries will be interested to build the VIRYA-3.6PC. But as the possibilities of manufacture in these countries will be limited, the pitch control system must be as simple and as cheap as possible. The following choices were made.

1 A rotor with three blades is used. The main advantage of a 3-bladed rotor is that the gyroscopic moment in the rotor shaft isn't fluctuating. A 2-bladed rotor with 7.14 % cambered blades and a design tip speed ratio of 4.5 would have rather wide blades and generally a 3-bladed rotor is found more beautiful than a 2-bladed rotor. A pitch control system for a 3-bladed rotor is more complicated than for a 2-bladed rotor but the chosen system seems simple enough if one has the required machines.

2 Positive pitch control, activated by only the aerodynamic moment, will be used. So no centrifugal weights will be used like it is often done for pitch control systems of small wind turbines. The axis of the blade shaft will be chosen as close as possible to the quart chord point of the airfoil.

3 The blade shaft will be made of bare drawn stainless steel bar round 20 mm h9 with a length of 665 mm. So nine blade shafts can be made from 6 m shaft. The outer side of the blade shaft is welded to the cambered blade strip. It is assumed that needle bearings can run directly on the blade shaft. A threaded hole M12 is made at the inner side of the blade shaft and the centrifugal force is taken by a hexagon bolt M12 * 30 mm. The blade shaft is turning into two sealed needle bearings size $\phi 20 * \phi 26 * 20$ mm. A needle bearing is pressed into a stainless steel bearing housing size 20 * 40 * 70 mm. A bearing housing is bolted to the hub plate by two inner hexagon bolts M12 * 60.

4 The centrifugal force in the blade is rather high for the rotational speed for which the blade starts pitching. To minimise friction, a stainless steel thrust ball bearing size $\phi 20 * \phi 35 * 10$ mm is used to take the centrifugal force. The thrust bearing pushes to one side of the inner bearing housing. A stainless steel ring size $\phi 30 * 5$ mm is used in between the thrust bearing and the M12 bolt head. As the thrust bearing isn't sealed, a stainless steel bearing should be used.

5 There is no synchronisation mechanism which makes that the variation of the blade angle is exactly the same for both blades. This makes the system rather simple. A lever is clamped around each blade shaft by an inner hexagon bolt M12 * 40 shortened to 39 mm. A torsion spring pushes the outside part of the lever against the hub plate. The torsion spring is mounted around the blade shaft. As the lever can be clamped in any position, a blade should be adjusted such that the normal blade angle $\beta = 8°$.

6 The pitch movement starts at a loaded rotational speed of 210 rpm. This rotational speed corresponds to the working point for a wind speed of 8 m/s (see figure 4). For this working point, the rotor is turning at a somewhat higher tip speed ratio than $\lambda_d = 4.5$. Using formula 8, it can be calculated that this corresponds to a tip speed ratio $\lambda = 4.95$.

7 The blade can rotate over 30°. In chapter 3 it was calculated that the optimum blade angle $\beta = 8°$. So the maximum blade angle will be $\beta_{max} = 38°$. These two angles are realised by the shape of the lever to which the torsion spring is connected. The outer bottom side of the lever makes contact with the hub plate for $\beta = 8°$. The inner bottom side of the lever makes contact with the hub plate for $\beta = 38°$. It is expected that $\beta_{max} = 38°$ results in a reduction of the tip speed ratio which is enough to effectively limit the rotational speed of the rotor, even for very high wind speeds.

8 The shape of the torsion spring is chosen such that both straight ends are lying in one plane. This means that the blade shaft can be mounted on the hub plate without stress in the spring. Next the inner side of the spring is rotated about 10° and hooked behind the M8 bolt at the lever. Next the outer side of the spring is rotated over about 185° and hooked behind a hook which is mounted at the side of the hub plate. So the total angle of rotation $\gamma$ of the torsion spring is 195° for $\beta = 8°$ and 225° for $\beta_{max} = 38°$.

9 A 2 mm bronze ring is mounted in between the lever and the inner bearing housing. So the lever has also a function to prevent that the blade shaft can move to the inside by the blade weight if the rotor isn't rotating and if the blade is in the upwards position.

10 The triangular hub plate is made of 6 mm stainless steel sheet and mounted to the hub by three inner hexagon bolts M12 * 80. The pitch circle of these bolts is 58 mm. The eccentricity in between the blade axis and the centre of the hub plate is 60 mm. The length of each ear of the hub plate to a heart line through the centre of the hub plate is 200 mm. The eccentricity in between the blade shaft and the centre of the hub plate is 60 mm.

11 The hub is made of 80 mm stainless steel bar with a length of 58 mm with a tapered central hole. The hub is pulled on the tapered 35 mm shaft of the PM-generator by one central inner hexagon bolt M16 * 40.

A sketch of the pitch control mechanism of the VIRYA-3.6PC is given in figure 6.

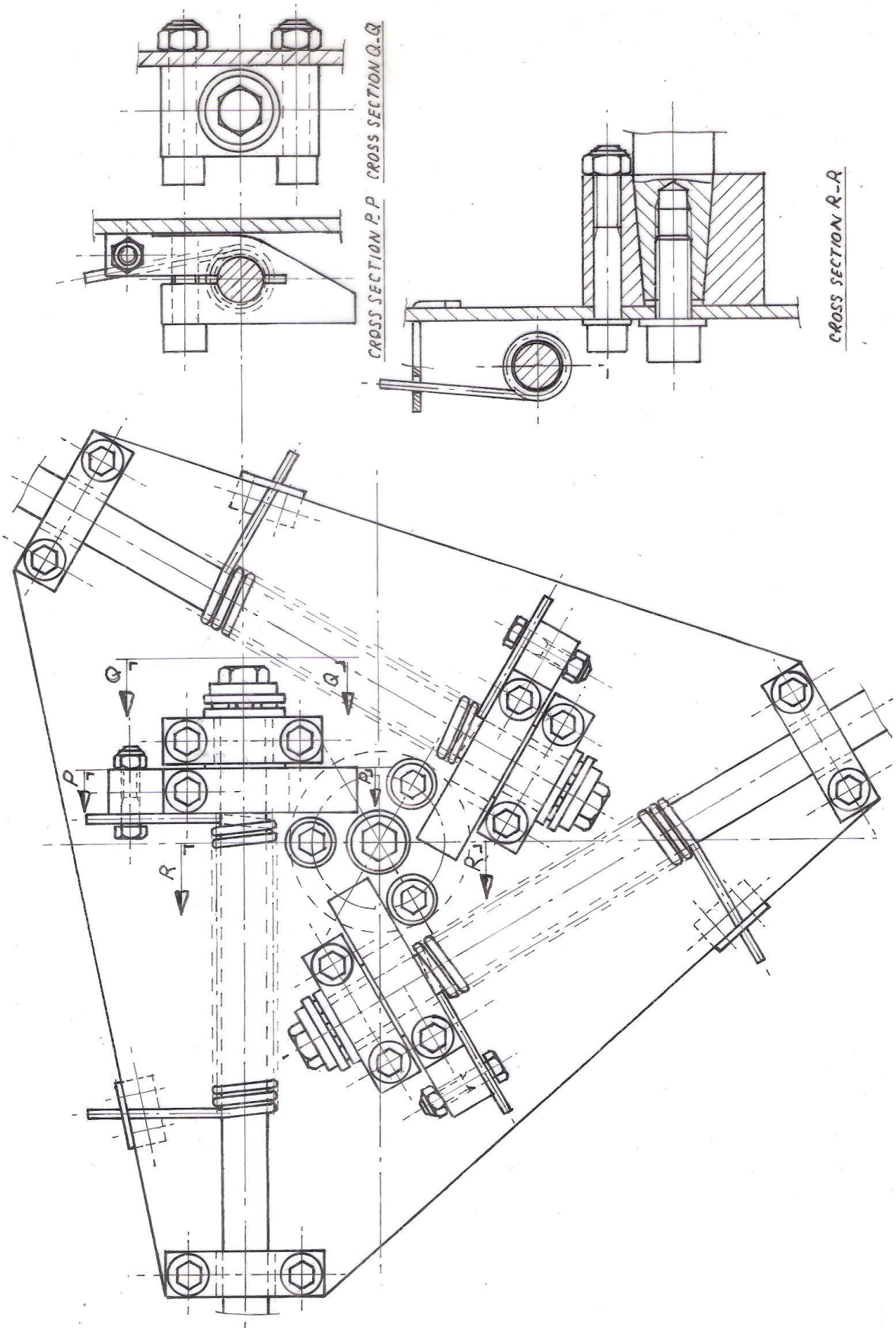


fig. 6 Pitch control mechanism VIRYA-3.6PC

### 6.3 Determination of the aerodynamic moment

The aerodynamic moment M depends on the aerodynamic moment coefficient $C_m$, the blade dimensions and the relative wind speed W which is felt by the blade. The characteristics of the 7.14 % cambered airfoil as given in KD 398 (lit. 3), have originally been measured by Buering of Imperial College. Unfortunately he didn't measure the aerodynamic moment coefficient $C_m$. However, the aerodynamic moment coefficient has been measured by Flachsbart for blades with an aspect ratio of 5 and for 5 % and 10 % camber. In my report KD 501 (ref. 7), I have derived the $C_{m0.25}$-$\alpha$ curve for 7.14 % camber by taking the average of the $C_{m0.25}$-$\alpha$ curves for 5 % camber and 10 % camber. The real blade has an aspect ratio of 6 so it is assumed that the values for an aspect ratio of 5 can be used. The estimated $C_{m0.25}$-$\alpha$ curve for 7.14 % camber is given in figure 4 of KD 501. The direction of M is chosen such that M is positive for the right hand direction, so for a direction which results in increase of the angel of attack $\alpha$. In figure 4 of KD 501 it can be seen that the $C_{m0.25}$ value is about constant and about 0.18 for $0° < \alpha < 12°$. In table 1 it can be seen that the linearised angle of attack $\alpha_{lin}$ varies in between 0.4° at station A and 11.4° at station J. So it is allowed to calculate with a constant value of $C_{m0.25} = 0.18$. This is favourable because it simplifies the calculation of M.

The aerodynamic moment around the quart cord point, $M_{0.25}$ is given by:

$$M_{0.25} = C_{m0.25} * ½\rho W^2 * c^2 * b \qquad \text{(Nm)} \qquad (10)$$

In this formula, b is the airfoil width. Formula 10 is only valid if the airfoil is streamed by a wind speed W which is the same for the whole airfoil width. This is not the case for a rotating windmill blade. In this case the relative wind speed W, which is felt by the blade, differs for each station. If the wake rotation is neglected, W is given by formula 5.12 of KD 35. This formula is copied as formula 11.

$$W = V \sqrt{(\lambda_{rd}^2 + 4/9)} \qquad \text{(m/s)} \qquad (11)$$

This formula is correct if the rotor is turning at the design tip speed ratio $\lambda_d$. However, at V = 8 m/s, the rotor is not turning with $\lambda_d = 4.5$ but with $\lambda = 4.95$ which is a factor 1.1 higher. So the local design tip speed ratios $\lambda_{rd}$ as given in table 1 have to be multiplied by a factor 1.1 to find the real local tip speed ratio $\lambda_r$. Next the blade is divided into five sections 1 to 5 starting at the blade tip and each having a width b = 0.24 m. The relative wind speed is calculated for the middle of a section, so for cross sections B, D, F, H and J and it is assumed that this wind speed can be used for the whole section. The values of $\lambda_{rd}$ for a certain value of r can be derived from table 1. So the hart of section 1 corresponds to station B with r = 1.68 m and $\lambda_{rd} = 4.2$. The five sections and corresponding values of r, $\lambda_{rd}$ and $\lambda_r$ are given in table 3.

| Section | r (m) | $\lambda_{rd}$ (-) | $\lambda_r$ (-) | W (m/s) for V = 8 m/s | $M_{0.25}$ (Nm) |
|---|---|---|---|---|---|
| 1 | 1.68 | 4.2 | 4.62 | 37.34 | 1.520 |
| 2 | 1.44 | 3.6 | 3.96 | 32.13 | 1.125 |
| 3 | 1.20 | 3 | 3.3 | 26.93 | 0.790 |
| 4 | 0.96 | 2.4 | 2.64 | 21.78 | 0.517 |
| 5 | 0.72 | 1.8 | 1.98 | 16.71 | 0.304 |

table 3 r, $\lambda_{rd}$, $\lambda_r$, W and $M_{0.25}$ as a function of the section number

W is calculated for a wind speed V = 8 m/s. Substitution of V = 8 m/s and $\lambda_{rd} = \lambda_r$ in formula 11 gives:

$W = 8 \sqrt{(\lambda_r^2 + 4/9)}$ (m/s) (for V = 8 m/s) (12)

The calculated values of W are also given in table 4. Substitution of $C_{m0.25} = 0.18$, $\rho = 1.2$ kg/m$^3$, c = 0.205 m and b = 0.24 m in formula 10 gives:

$M_{0.25} = 0.00109 * W^2$ (Nm) (for V = 8 m/s) (13)

Next $M_{0.25}$ is calculated for each section for the values of W given in table 3 using formula 13. The calculated values of $M_{0.25}$ are also given in table 4. The total aerodynamic moment $M_{tot}$ is the sum of all calculated values of $M_{0.25}$.

So $M_{tot} = \Sigma M_{0.25}$ (Nm) (for V = 8 m/s) (14)

So $M_{tot} = 1.520 + 1.125 + 0.790 + 0.517 + 0.304 = 4.256$ Nm = 4256 Nmm

$M_{tot}$ at V = 8 m/s must be equal to the spring moment M of the torsion spring for $\beta = 8°$. The geometry of the torsion spring is determined in chapter 6.5.

**6.4 Checking of the load on the needle bearings and the thrust bearing**

A rotor blade is loaded in the axial direction by a bending moment which is caused by the rotor thrust or by the gyroscopic moment. A rotor blade is also loaded by its own weight in the tangential direction but the influence of this load is neglected. As the head is turned on the wind by a double vane (see chapter 7), the head rotation is rather slow and the gyroscopic moment can therefore be neglected. The rotor thrust $F_t$ is given by formula 4.12 of KD 35 which is copied as formula 15.

$F_t = C_t * ½\rho V^2 * \pi R^2$ (N) (15)

Formula 15 gives the rotor thrust on the whole rotor. The rotor thrust on one blade of a rotor with three blades $F_{t\,bl}$ is 1/3 of the thrust on the whole rotor, so:

$F_{t\,bl} = 0.3333 * C_t * ½\rho V^2 * \pi R^2$ (N) (16)

The thrust coefficient for the VIRYA-3.6PC rotor is about 0.7 if the rotor runs at $\lambda_d = 4.95$. $F_{t\,bl}$ is calculated for the same wind speed which was also used to calculate $M_{tot}$, so V = 8 m/s. Substitution of $C_t = 0.7$, $\rho = 1.2$ kg/m$^3$, V = 8 m/s and R = 1.8 m in formula 16 gives that $F_{t\,bl} = 91$ N. The distribution of the thrust over the rotor blade has about the shape of a triangle with the highest value at the blade tip. A triangle load gives a bending moment $M_b$ at the hart of the rotor which is the same as the moment of a point load at 2/3 R. To simplify the calculation, it is assumed that the real thrust distribution can be replaced by a point load at 2/3 R, so at $r_t = 1.2$ m.

The blade shaft is supported in two INA needle bearings. Bearing no 1 is the outer bearing and bearing no 2 is the inner bearing. It is expected that the distance in between the heart of bearing no1 and the heart of bearing no 2 is 0.235 m. The distance a in between $r_t$ and the heart of bearing no 1 is 1.01 m. The distance b in between $r_t$ and the heart of bearing no 2 is 1.245 m.

The reaction force $F_1$ at bearing no 1 can be calculated by taking the balance of moments around bearing no 2. This gives:

$$F_1 = F_{t\,bl} * b / (b - a) \qquad (N) \qquad (17)$$

Substitution of $F_{t\,bl}$ = 91 N, b = 1.245 m and a = 1.01 m in formula 17 gives $F_1$ = 482 N.

The reaction force $F_2$ on bearing no 2 is given by:

$$F_2 = F_1 - F_{t\,bl} \qquad (N) \qquad (18)$$

Substitution of $F_1$ = 482 N and $F_{t\,bl}$ = 91 N in formula 18 gives $F_2$ = 391 N. The direction of $F_1$ is frontwards but the direction of $F_2$ is backwards. The blade will bend somewhat backwards because of the thrust and this results in a counteracting moment due to the centrifugal force in the blade. This counteracting moment reduces the bending moment in the blade and therefore the forces $F_1$ and $F_2$ are also reduced somewhat. But this effect on $F_1$ and $F_2$ is neglected.

The sealed needle bearings are given in the Dutch INA catalogue no 307 at page 124. The inside diameter is 20 mm. The outside diameter is 26 mm. The width is 20 mm. The code number is HK 2020.2RS. The rotational speed of the bearings is very small so the bearing is calculated for static conditions. The static load factor is 20100 N. This is very much larger than the calculated load of 482 N for bearing no 1. Normally a needle bearing is used on a hardened shaft. For the VIRYA-3.6PC it is used on a bare drawn stainless steel shaft which isn't hardened but I think that this is allowed because of the very low load compared to the static load factor of the bearing.

The thrust ball bearing has an inner diameter of 20 mm, an outer diameter of 35 mm and a thickness of 10 mm. The bearing code is 51104. As the bearing isn't build in and protected against weather influences, one should use a stainless steel version. The rotational speed will be very low so the strength of the bearing is checked for the static load factor $C_0$. $C_0$ = 16600 N for this bearing.

The bearing will be loaded by the centrifugal force in the blade. The centrifugal force is the sum of the centrifugal force acting on the blade, the cambered blade strip and the blade shaft. The cross sectional area of the blade is 624 $mm^2$. The cross sectional area of the blade shaft is 314 $mm^2$, so much smaller. To simplify the calculation it is assumed that the blade has a length of 1.5 m and that only the blade mass is taken into account. The mass m of this blade is 7.3 kg. The centrifugal force $F_c$ will be calculated for the blade mass concentrated in the centre of gravity of the blade. So the radius of the centre of gravity $r_c$ is given by:
$r_c = 1.8 - 0.5 * 1.5 = 1.05$ m. $F_c$ is given by:

$$F_c = m * r_c * \Omega^2 \qquad (N) \qquad (19)$$

The centrifugal force will be calculated for a rotational speed n = 210 rpm, belonging to the design point for a wind speed of 8 m/s. This gives an angular velocity $\Omega = \pi * 210 / 30 =$ 22 rad/s. Substitution of m = 7.3 kg, $r_c$ = 1.05 m and $\Omega$ = 22 rad/s in formula 19 gives that $F_c$ = 3710 N. So the load is much lower than the static load factor $C_0$ = 16600 N and the bearing is therefore strong enough.

The two needle bearings and the thrust bearing have very low friction and therefore only a little hysteresis may be active for the blade movement as a function of the variation of the rotational speed.

### 6.5 Determination of the torsion spring geometry

In chapter 6.3 it has been determined that the torsion spring must have a moment M = 4256 Nmm for a blade angle $\beta = 8°$. In point 7 of chapter 6.2 is was assumed that the blade can rotate over 30° and so the maximum blade angle $\beta_{max} = 38°$. The angle of rotation of the torsion spring is called $\gamma$. In point 8 of chapter 6.2 it was assumed that $\gamma = 195°$ for $\beta = 8°$. So $\gamma = 225°$ for $\beta_{max} = 38°$. The spring moment M increases linear to the angle of rotation $\gamma$, so it is 4256 * 225 / 195 = 4911 Nmm for $\gamma = 225°$.

So the spring moment increases by a factor 225 / 195 = 1.154 if the blade moves from $\beta = 8°$ to $\beta_{max} = 38°$. The aerodynamic moment increases proportional to the square of the rotational speed if the moment coefficient is constant. This means that the rotational speed has to increase only by a factor $1.154^{1/2} = 1.074$ to reach the maximum blade angle $\beta_{max} = 38°$. So the safety system is reacting very sensible to a little over speed and in practice it can be assumed that the rotational speed is kept almost constant above wind speeds of 8 m/s.

The spring geometry is calculated using formulas given in chapter 10.1 of the blue (about 1990) catalogue of the Dutch spring manufacturer Hengelose Verenfabriek Bakker BV (ref. 8). The current name of this company is United Springs BV. In this catalogue, the angle of rotation of the torsion spring is called $\alpha$ but I use $\gamma$ as $\alpha$ is already used for the angle of attack. The following formulas are used in the catalogue to calculate a torsion spring (draaiveer in Dutch).

$$\sigma_b = 10.2 * M / d^3 \quad (N/mm^2) \tag{20}$$

$$C = E * d^4 / (1170 * l) \quad (Nmm/degree) \tag{21}$$

Formula 21 can be written as:

$$l = E * d^4 / (1170 * C) \quad (mm) \tag{22}$$

$$C = M / \gamma \quad (Nmm/degree) \tag{23}$$

$$D = l / (\pi * n) \quad (mm) \tag{24}$$

Formula 24 can be written as:

$$n = l / ( \pi * D) \tag{25}$$

In these formulas $\sigma_b$ is the bending stress ($N/mm^2$), M is the torsion moment (Nmm), d is the wire thickness (mm), C is the spring constant (Nmm/degree), E is the modulus of elasticity of the used spring material ($N/mm^2$), l is the material length of the windings of the torsion spring (mm), n is the number of windings (-), L is the length of the spring, $\gamma$ is the angle of rotation (°) and D is the diameter of the spring at the pitch circle (mm).

Apart from these six formulas, the catalogue also shows figure 1 which gives a nomograph to estimate the wire thickness d for a certain torsion moment M, figure 2 which gives the allowable bending stress depending on the spring material and the wire thickness and figure 3 which gives the correction factor q for the bending stress $\sigma_b$ as a function of the ratio D/d.

One starts with the nomograph to estimate the wire thickness. For M = 4911 Nmm it can be read that d = 4.1 mm. Assume d = 4 mm. Substitution of M = 4911 Nmm and d = 4 mm in formula 20 gives that $\sigma_b = 783$ $N/mm^2$. Assume we use stainless spring steel. In figure 2 of the catalogue it can be read that the allowable stress is 1080 $N/mm^2$ for stainless spring steel with a diameter of 4 mm.

However, this value still has to be corrected once the ratio D/d is known. Substitution of M = 4911 Nmm and $\gamma = 225°$ in formula 23 gives that C = 21.83 Nmm/degree. The modulus of elasticity E of stainless steel spring steel is about 200000 N/mm$^2$. Substitution of E = 200000 N/mm$^2$, d = 4 mm and C = 21.83 Nmm/degree in formula 22 gives that l = 2005 mm.

The length of the spring L for a certain wire length l now depends on the diameter D and on the distance a in between the windings. The diameter D must be chosen such that the torsion spring fits around the 20 mm blade shaft. This means that the inside diameter of the spring must be at least 21 mm. Assume D = 25 mm. This gives an inside diameter of 21 mm for a wire thickness d = 4 mm. Substitution of l = 2005 mm and D = 25 mm in formula 25 gives that n = 25.5 windings rounded to n = 26 windings.

Assume that the distance a in between the windings is chosen 1 mm. The spring length L for one winding is two times the wire thickness d plus one time the distance a. So for 26 windings, the spring length L becomes (26 + 1) * 4 + 26 * 1 = 27 * 4 + 26 * 1 = 134 mm.

Next the bending stress is checked for the chosen spring diameter. D = 25 mm and d = 4 mm give that D / d = 6.25. In figure 3 of the catalogue it can be seen that q = 1.22 for D / d = 6.25. So the real bending stress is 1.22 * 783 = 955 N /mm$^2$. The allowable stress for 4 mm stainless spring steel is 1080 N/mm$^2$ so the spring is strong enough. Another point is that the spring is calculated for the maximum torsion angle $\gamma = 225°$ and that normally the torsion angle will be smaller which also results in a lower stress. The spring stress is varying only a little in between $\gamma = 195°$ and $\gamma = 225°$ and the number of oscillations will also be small so I think that the spring isn't sensible for fatigue.

## 7 Description of the vane

The head must be turned into the wind. This yawing of the head around the tower axis causes a gyroscopic moment perpendicular to the plane of the rotor axis and the tower axis. The direction of the gyroscopic moment depends on the direction of rotation of the rotor shaft and of the direction of rotation of the head along the tower axis. The rotor turns always in the same direction but the yawing along the tower axis is half the time left hand and half the right hand. So the gyroscopic moment has half the time a tendency to push the rotor down and half the time to lift the rotor up. The gyroscopic moment in the blades and in the rotor shaft is maximal for the blades in vertical position and zero for the blades in horizontal position if the rotor has two blades. The gyroscopic moment is proportional to the angular velocity of the rotor, the angular velocity of the yaw movement and the moment of inertia of the rotor. So to limit the fluctuation of gyroscopic moment it is important that yawing takes place only slowly.

A normal vane will turn the head too fast at high wind speeds. A system with side rotors which drive the head in the wind through a reducing gearing gives a very low yawing speed around the tower axis but this system is rather complicated and expensive. I have tested a so called double vane system on one of my earliest windmills, the DRIEKA-4, which had a rotor diameter of 4 m and a (very noisy) safety system with elastic air brakes on the blade tips. It was equipped with a 6 m long horizontal pipe parallel to the rotor plane with a square sheet on each end of the pipe. Each sheet makes an angle of 20° with the rotor axis and the direction of the angles is chosen such that touching lines along the sheets intersect with the rotor axis before the rotor. Each sheet had a width and height of 500 mm and was made of 4 mm steel sheet. A photo of the DRIEKA-4 is given in figure 10. It is expected that the same vane geometry can be used for the VIRYA-3.6PC but it might also be possible to use a 5 m or 4 m long pipe in stead of a 6 m long pipe to reduce the overall vane dimensions.

fig. 10 The DRIEKA-4 windmill with double vane and tree tower designed in about 1985

The moment of inertia of this vane is very large and fast head movements are therefore damped very well. The optimum position of the pipe might be at the back side of the head frame just as it was also done for the DRIEKA-4. For this position, there is about balance of the vane weight and the weight of the generator and the rotor and this means that the moment on the yaw bearing housing is minimal.

If the VIRYA-3.6PC rotor is used in combination with a centrifugal pump, a rotating shaft in the tower and an accelerating rectangular gear box in the tower top, the vertical shaft will give a certain reaction torque on the head making that the rotor will not be perpendicular to the wind. This reaction torque can be compensated by using two different angles for the vane blades for instance 25° at one blade and 15° at the other blade. The correct angles have to be calculated when the reaction torque is known.

I won't build the VIRYA-3.6PC myself. May be I will make detailed drawings of the rotor in future. I have the generator and the tower of the VIRYA-4.2 available. I also have a 550 W dump load and a 28 V battery charge controller to simulate a 24 V battery. If someone builds the rotor and the head, the existing components can be used to test a prototype on my test field. The VIRYA-4.2 generator and tower are also for sale.

## 8 References


1 Kragten A. Measurements performed on a generator with housing 5RN112M04V and a 4-pole armature equipped with neodymium magnets, June 2004, reviewed September 2004, free public report KD 200, engineering office Kragten Design, Populierenlaan 51, 5492 SG Sint-Oedenrode, The Netherlands.

2 Kragten A. Development of the VIRYA-3.6, a windmill with a Polycord transmission in between the rotor and the vertical shaft to drive a standard centrifugal pump, April 2018, free public report KD 653, engineering office Kragten Design, Populierenlaan 51, 5492 SG Sint-Oedenrode, The Netherlands.

3 Kragten A. Development of a tubular tower for the VIRYA-4.2 and the VIRYA-4.6B2, March 2015, reviewed November 2016, free public report KD 582, engineering office Kragten Design, Populierenlaan 51, 5492 SG Sint-Oedenrode, The Netherlands.

4 Kragten A. The 7.14 %, 10 % and 12.5 % cambered plate as airfoil for windmill rotor blades, Aerodynamic characteristics, geometry, moment of inertia I and moment of resistance W, November 2002, free public report KD 398, engineering office Kragten Design, Populierenlaan 51, 5492 SG Sint-Oedenrode, The Netherlands.

5 Kragten A. Rotor design and matching for horizontal axis wind turbines, January 1999, reviewed February 2017, free public report KD 35, engineering office Kragten Design, Populierenlaan 51, 5492 SG Sint-Oedenrode, The Netherlands.

6 Kragten A. Determination of $C_q$ for low values of $\lambda$. Deriving the $C_p$-$\lambda$ and $C_q$-$\lambda$ curves of the VIRYA-1.8D rotor, July 2002, free public rapport KD 97, engineering office Kragten Design, Populierenlaan 51, 5492 SG Sint-Oedenrode, The Netherlands.

7 Kragten A Determination of the $C_m$-$\alpha$ curves for different positions of the axis of rotation for a 10 %, 5 % and 7.14 % cambered airfoil with an aspect ratio of 5, July 2012, reviewed April 2018, free public report KD 501, engineering office Kragten Design, Populierenlaan 51, 5492 SG Sint-Oedenrode, The Netherlands.

8 Blue catalogue Hengelose Verenfabriek Bakker (current name United Spring BV), date probably about 1990, Petroleumhavenstraat 14, P.O. box 50, 7550 AB Hengelo, the Netherlands, telephone 074 2555444, website: https://www.twentekanaal.com .